the outflow in the Atlantic cannot be eastward along the equatorial corridor because there is no direct oceanographic connection. Instead, these warm saline waters flow eastward into the western boundary current of the North Atlantic subtropical gyre and are delivered into the subpolar Atlantic, producing the rapid melting of ice and hence Heinrich events. This is a seasonal process. From inflection points to maxima, there is a diminution in the zonal component relative to the meridional component of the tropical easterlies in the key season of Northern Hemisphere summer. Relaxation of the zonal force permits increasing amounts of heat and salt to flow eastward into the western boundary current, culminating in *F. profunda* maxima and Heinrich events. This mechanism alters the partitioning of heat loss from these inland seas. Latent heat flux to the atmosphere decreases relative to sensible heat loss to the North Atlantic Ocean by means of surface water advection as the zonality of tropical easterlies decreases; the opposite effect occurs as the zonality increases.

The mechanism that we propose for the delivery of heat- and salt-enhancing or -retarding continental ice accumulation and sea ice–ocean density stratification is complimentary to the "binge and purge hypothesis" (*26*), to the "conveyer belt hypothesis" (*25*), and to the evidence that variation in the advection of warm Atlantic surface water into the Norwegian Sea influenced both atmospheric circulation through the last glacial-interglacial transition (*27*) and Greenland ice for 0 to 41 ka (*2*). Our results also support the initial view that Heinrich events were a product of precessional forcing (*1*). Circumstantial evidence exists in the correlation between Heinrich events and similar millennial-scale responses in the Greenland ice (*19*) and with spectral analyses of Vostock (Antarctica) and GRIP (Greenland) ice cores, which contain stable spectral peaks at 8.96 and 7.76 ky, respectively (*28*).

If our scenario is correct, then at ~3 ^{14}C ka, equivalent to ~3 ka (α in Fig. 1C), the modality of the system changed. During this time, there was a concomitant increase in precipitation around the North Atlantic in subpolar latitudes and a decrease in precipitation in West Africa (*29–32*). The precessional forcing and response mechanism described here will continue to at least 28,000 A.D.; consequently, *F. profunda* maxima should occur at ~3200 A.D. and ~11,600 A.D.

REFERENCES AND NOTES

1. H. Heinrich, *Quat. Res.* **29**, 143 (1988).
2. P. Mayewski *et al.*, *Science* **263**, 1747 (1994).
3. A. T. Kotilainen and N. J. Shackleton, *Nature* **377**, 323 (1995); E. C. Grimm, G. L. Jacobson Jr., W. A. Watts, B. C. S. Hansen, K. A. Maasch, *Science* **261**, 198 (1993).
4. B. Molfino and A. McIntyre, *Science* **249**, 766 (1990).
5. A. McIntyre *et al.*, *Paleoceanography* **4**, 19 (1989); A. McIntyre *et al.*, *Program for the Fifth International Conference on Paleoceanography* (Halifax, Nova Scotia, 1995), p. 54.
6. D. J. Verardo and A. McIntyre, *Paleoceanography* **9**, 63 (1994).
7. G. Reverdin, in *Upwelling in the Ocean: Modern Processes and Ancient Records*, C. P. Summerhayes *et al.*, Eds. (Wiley, New York, 1995), pp. 125–148.
8. R. H. Weisberg and T. Y. Tang, *J. Geophys. Res.* **92**, 3709 (1987).
9. G. A. Jones, *Deep-Sea Res.*, in press.
10. G. M. Jenkins and D. G. Watts, *Spectral Analysis and Its Applications* (Holden-Day, Oakland, CA, 1968). All spectra are linear variances of time series calculated by standard time series procedures at the 95% confidence interval: linear detrending; prewhitening (0.8); autocovariance function; Tukey-Hanning lag window ($M = n/3$); time interval, 0.3 ky, and a fixed n (132 for ^{14}C and 147 for calendric signals) for all three cores.
11. E. N. Lorenz, *Meteorol. Monogr.* **8**, 1 (1968).
12. L. D. Keigwin and G. A. Jones, *Paleoceanography* **10**, 973 (1995).
13. T. Fronval *et al.*, *Nature* **374**, 443 (1995).
14. S. C. Porter and A. Zhisheng, *ibid.* **375**, 305 (1995).
15. M. Stuiver and P. J. Reimer, *Radiocarbon* **35**, 215 (1993).
16. E. Bard *et al.*, *ibid.*, p. 191.
17. Test of symmetry of a random variable Y about a point c. If we assume that Y has a frequency function p, then symmetry about c is $p(Y + c) = p(Y - c)$. P. J. Bickel and K. A. Doksum, *Mathematical Statistics* (Holden-Day, Oakland, CA, 1977).
18. Calendric chronology of cores RC2402 and RC2408 yields eight peak-to-peak intervals having a range of 8.1 to 9.0 ky, with a mean of 8.43 ky.
19. G. C. Bond and R. Lotti, *Science* **267**, 1005 (1995).
20. D. A. Short *et al.*, *Quat. Res.* **35**, 157 (1991).
21. T. K. Hagelberg *et al.*, *Paleoceanography* **9**, 545 (1994).
22. The error of estimate in years for the AMS ^{14}C chronology ranges from ±30 to ±420 for dated samples, but for interpolated values we consider that these estimates could be larger as a result of variation in sedimentation rate. However, in RC2408, *F. profunda* maxima were either directly AMS-dated or have dates closely allied with them. Calendric conversion yields 2σ errors ranging from ±35 to ±450. We found that the extreme case for the oldest peak-to-peak interval for conversion (*15*), using a minus error for the younger peak and a plus error for the older peak, is 8.75 ky. The estimate of the oldest interval for conversion (*16*) is 9.3 ky.
23. A. Berger, *Quat. Int.* **2**, 1 (1989); P. I. Pestiaux *et al.*, *Clim. Change* **12**, 9 (1988).
24. A. Berger and M. F. Loutre, *Sci. Rep. Inst. Astron. Geophys.* **13**, 1 (1988).
25. W. S. Broecker *et al.*, *Clim. Dyn.* **6**, 265 (1992).
26. H. Haflidason *et al.*, *Geology* **23**, 1059 (1995).
27. D. R. MacAyeal, *Paleoceanography* **8**, 775 (1993).
28. P. Yiou *et al.*, *Geophys. Res. Lett.* **22**, 2175 (1995).
29. B. Fontaine and S. Bigot, *Int. J. Climatol.* **13**, 271 (1993).
30. F. Gasse and E. vanCampo, *Earth Planet. Sci. Lett.* **126**, 435 (1994). Evidence of increased drought in West Africa at ~4 to 3 ka is presented.
31. D. A. Hodell *et al.*, *Nature* **375**, 391 (1995). In their figure 2, there is a marked change in lithic-chemical-isotope character of the lake sediments at ~3 ka (^{14}C years) in Central America.
32. S. P. Harrison *et al.*, *Quat. Res.* **45**, 138 (1996); S. O. Dahl and A. Nesje, *Holocene* **3**, 269 (1993). Increased precipitation is inferred from changes in vegetation and lake levels and glacial accretion on the continents adjacent to the subpolar North Atlantic after 5 ka.
33. We thank M. Yarusinski for assistance. Supported by NSF [MG&G grant OCE93-13821 (95%)], and NSF OCE801015 AMS/National Ocean Sciences Accelerator Mass Spectrometry Facility. This is Lamont-Doherty Earth Observatory contribution 5579.

9 July 1996; accepted 25 September 1996

Latest *Homo erectus* of Java: Potential Contemporaneity with *Homo sapiens* in Southeast Asia

C. C. Swisher III, W. J. Rink, S. C. Antón, H. P. Schwarcz, G. H. Curtis, A. Suprijo, Widiasmoro

Hominid fossils from Ngandong and Sambungmacan, Central Java, are considered the most morphologically advanced representatives of *Homo erectus*. Electron spin resonance (ESR) and mass spectrometric U-series dating of fossil bovid teeth collected from the hominid-bearing levels at these sites gave mean ages of 27 ± 2 to 53.3 ± 4 thousand years ago; the range in ages reflects uncertainties in uranium migration histories. These ages are 20,000 to 400,000 years younger than previous age estimates for these hominids and indicate that *H. erectus* may have survived on Java at least 250,000 years longer than on the Asian mainland, and perhaps 1 million years longer than in Africa. The new ages raise the possibility that *H. erectus* overlapped in time with anatomically modern humans *(H. sapiens)* in Southeast Asia.

The geologic age and taxonomic affinity of hominid fossils from Ngandong and Sambungmacan, Central Java, bear directly on the controversy surrounding the origin of anatomically modern humans (*H. sapiens*). Proponents of a regional continuity model for the origin of *H. sapiens* consider that these fossils are both morphologically and temporally transitional between Javanese *H. erectus*, such as Sangiran 17, that are older than 780,000 years ago (ka), and early robust Australian *H. sapiens*, such as Willandra Lakes Hominid (WLH) 50, that first appear about 30 ka (*1*, *2*). The opposing view is that *H. sapiens* arose in Africa less than 200 ka and only recently spread out over Europe and Asia, replacing existing populations of hominids with little or no interbreeding (*3–5*). Both views recognize strong morphological continuity between mid-Pleistocene Javanese *H. erectus* and the Ngandong and Sambungmacan hominids, but differ in how these hominids relate to *H. sapiens* (*1, 3, 6, 7*). Here, we present geochronological data that suggest that *H. erectus* persisted in Southeast Asia much longer than in either Africa or mainland Asia, and may have coexisted in time with *H. sapiens*.

Hominid fossils were discovered at Ngandong in 1931, 40 years after the discovery of the type *H. erectus* specimen at Trinil (Fig. 1). Between 1931 and 1933, the Dutch Geological Survey in Java conducted excavations in a 50 by 100 m area that yielded over 25,000 vertebrate fossils, including a total of 12 hominid calvaria and partial calvaria and two hominid tibiae (*8*). In excavations by Gadjah Mada University (GMU) between 1976 and 1980 in an adjacent 25 by 14 m area, an additional 1200 vertebrate fossils were recovered, including two partial hominid calvaria and hominid pelvic fragments (*9*). In both excavations, most of the 26,000 fossil vertebrates and all of the hominids were concentrated in an interval 50 cm or less thick near the base of a 0- to 3-m thick terrace deposit of the Solo River (Fig. 1) (*8*). The Ngandong terrace, also referred to as the High Terrace (*10*), is situated 20 m above the level of the present-day Solo River in the Kendeng Hills region and is traceable for some 15 km (*10*). The fossiliferous interval consists of volcaniclastic sandstone intermixed with marl cobbles from the unconformably underlying Pliocene Kalibeng Formation. Fossil accumulations at Ngandong, and in outcrops of the 20-m terrace deposit elsewhere, occur primarily at bends of the present-day Solo River (*11*), suggesting that the river had a similar course in the past and that the 20-m terrace is geomorphologically young.

The fragmentary nature of the fossils at Ngandong and their association with fluvial sediments suggest that they have been transported by water, although the presence in the nonhominid fossils of a few articulated vertebrae and a few crania with associated mandibles indicates that the amount of transport was minimal. Likewise, both hominid and nonhominid crania show little evidence of abrasion because fragile processes such as the pterygoid plates are preserved (*12*). Most of the fossils consist of isolated teeth, single and partial elements, and fragments (*8, 12*). Despite recent claims to the contrary (*6*), no complete skeletons were found (*13*). The lack of systematic study of the nonhominid fossils, rather than taphonomic processes, may explain why so few hominid postcranial elements (two tibiae and partial pelvic fragments) were reported from the Ngandong excavations because fragmentary hominid remains may have gone unidentified among the fauna (*6, 14*). Except for the few fossils described by von Koenigswald housed at the Geological Research and Development Center (GRDC), most of the 25,000 fossils from the original Dutch excavations appear to be lost (*15*).

Age estimates for the Ngandong fossil site have varied widely. Faunal correlations, as well as the geomorphology of the site, indicate that the fossil site is late Pleistocene in age (*8, 16*). However, a mid-Pleistocene age has been suggested for the hominids on the basis of morphological comparisons with *H. erectus* fossils elsewhere and because the hominids might have been reworked from older deposits into the late Pleistocene faunal assemblage (*6, 17*). All of the available evidence, however, indicates that the hominid and nonhominid faunas from Ngandong are of the same age. Photographs of Ngandong hominid calvaria V and VI show that the hominids were found in situ among the nonhomind fauna in the same Solo River terrace (*7, 8, 18*). Similar bone preservation and chemistry of the hominid and nonhominid fauna (*12, 19–21*) and the improbability of selectively reworking 15 hominids from the underlying marine marls or from upstream mammalian fossil-bearing exposures (the nearest located 30 km away) argue against any differential age sorting of the nonhominid and hominid fauna (*11*).

Radioisotopic ages reported for the Ngandong and Sambungmacan hominids are based on dates on volcanic rocks within the Notopuro (Pojajar) Formation at Sangiran (*22,23*). However, the fossil-poor Notopuro Formation has been shown to be older than the Solo River terraces (*10, 24, 25*). More recently, U-series dating of fossil bone chips from Ngandong have given ages between 31 and 101 ka (*10, 25*). Subsequent U-series dating of only the outer surface of the bone fragments yielded ages between 109 and 188 ka, whereas whole bone samples gave dates of 55 to 59 ka (*10, 25, 26*). These results showed that the outer surfaces of the bone had lost uranium long after uranium had been adsorbed by the bone and that ^{230}Th had grown partially into equilibrium with ^{234}U (*27*). Therefore, the true age may be younger than the whole bone analyses because these dates also incorporate a portion of the uranium-depleted bone (*26, 28*).

Our attempts to find primary volcanic material at Ngandong proved futile. ^{40}Ar/^{39}Ar analyses of detrital volcanic minerals collected from the overlying colluvium at the site gave dates ranging from over 400 to 100 ka (*29*), giving us a maximum age for the site. We decided to apply combined electron spin resonance (ESR) and U-series dating techniques to Ngandong fossil bovid tooth enamel (*30, 31*). We collected tooth samples from a 1-m-deep test pit in the terrace deposit at Ngandong, adjacent to the area quarried by Oppenoorth in the 1930s. At 220 cm below the present surface we encountered a zone consisting of volcaniclastic sandstone with cobbles of underlying Pliocene marl similar to that described by Oppenoorth as Layer 2 (Fig. 1). Much of

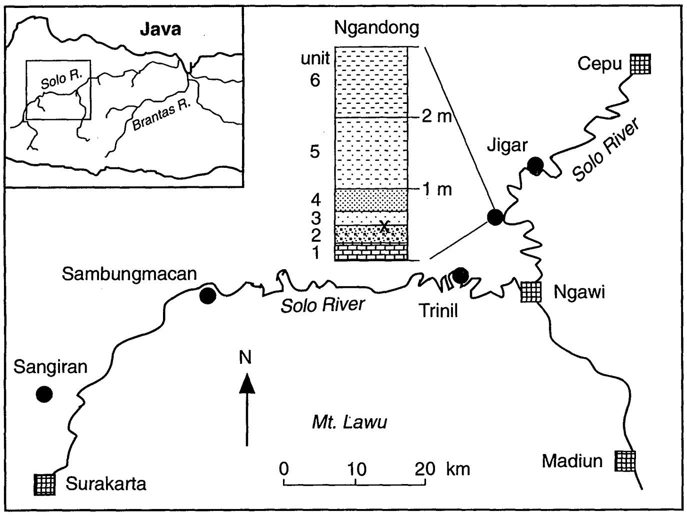

Fig. 1. Map showing location of the Ngandong, Sambungmacan, and Jigar sites, Central Java, Indonesia. At Ngandong, a general stratigraphic section, modified slightly from (*8*), is shown adjacent to the site. Hominid and nonhominid fossils (X) were recovered from Unit 2 in volcaniclastic sandstone with cobbles of underlying Pliocene marl. In our test pit, we were not able to distinguish Units 4 and 5, whereas Unit 6 is probably recent alluvium. Similar findings were reported by Bartstra *et al.* (*10*).

C. C. Swisher III and G. H. Curtis, Berkeley Geochronology Center, 2455 Ridge Road, Berkeley, CA 94709 USA.
W. J. Rink and H. P. Schwarcz, Department of Geology, McMaster University, Hamilton, Ontario, Canada L8S 4M1.
S. C. Antón, Department of Anthropology, University of Florida, Gainesville, FL 32611, USA.
A. Suprijo and Widiasmoro, Laboratory of Bioanthropology and Paleoanthropology, Gadjah Mada University, Yogyakarta, Indonesia, 55281.

the upper 2 m appeared to represent colluvium, possibly including some of the debris from the original 1930's quarry. Layer 2 was only about 30 cm thick in our test pit, but was found to contain numerous vertebrate fossils. We excavated three small pits 10 to 20 cm in diameter down through the 30-cm-thick interval. In two of the pits, we recovered well-preserved fossil bovid teeth (95296 and 95297). The teeth and the adjacent sediment were collected for ESR and U-series dating. Five dosimeters were placed into the wall of the excavation at and above the fossil-bearing layer for external dose rates and left in the site for 1 year (*32*). We also collected a bovid tooth (95301) and associated sediment from a test pit in a terrace deposit located approximately 7 km downstream from Ngandong near the village of Jigar where GMU had recovered abundant fossil vertebrates. The terrace deposit at Jigar (Fig. 1) is 19 m above the Solo River and its nonhominid fauna is considered to be similar to that of Ngandong (*33*).

To assure ourselves that we had excavated the same layer from which the Ngandong hominids were collected, we obtained bovid teeth from museum collections at GRDC and GMU. Bovid tooth GRDC 6679 was collected from Oppenoorth's layer 2, 15 February 1932, between the finds of Ngandong hominid calvaria IV (25 January 1932) and V (17 March 1932). A second bovid tooth was also obtained from the collections of the 1976–1980 GMU excavations from which Ngandong hominid calvarial fragments XIV and XV were discovered. The hominid calvaria and tibia from Sambungmacan (Fig. 1) are considered morphologically similar to the Ngandong hominids (*34*). Fluorine analyses of the Sambungmacan hominid tibia gave similar values as the nonhominid fauna, indicating that they are of similar age (*34 35*). We obtained a bovid tooth from the 1973 GMU excavation for direct age comparison with Ngandong.

ESR and U-series dating of bovid tooth enamel from Ngandong, Sambungmacan, and Jigar (Tables 1 and 2) was done at McMaster University following previously described preparatory and analytical methods (*30, 36, 37*). Two models of uranium uptake are generally considered in order to calculate an ESR age. In the early uptake (EU) model, it is assumed that all uranium in the tooth was adsorbed early in the burial history, whereas in the linear uptake (LU) model it is assumed that the uptake was continuous and constant throughout the burial history. The EU model yields the minimum age for a given data set provided that there has been no loss of uranium. LU-ESR ages have often agreed well with ages from other dating methods (*31*), although EU-ESR ages have been shown to agree well with radiocarbon and U-series ages in many geological settings (*38, 39*).

The teeth from all of the sites contained high concentrations of uranium (Tables 1 and 2). The dentine values are particularly high, and exceed values for any previously measured site of similar age (*40*). The EU-ESR ages are consequently significantly lower than the LU-ESR ages, although both models yield late Pleistocene ages. All of the teeth from the three separate excavations at Ngandong using either model give similar ages, indicating that the fossils from the site are of a single age and are not differentially reworked from older deposits. Similar ESR ages were obtained on Sambungmacan and Jigar teeth supporting the temporal correlation of these three sites (Table 1).

In order to evaluate the appropriate uranium uptake model for the dated teeth, we made mass-spectrometric U-series analyses of Ngandong enamels and dentine. Grün *et al.* (*41*) showed that, if early uptake of uranium had occurred, then the U-series and EU-ESR ages should agree, because all U-series ages are computed on the assumption that uranium uptake was early. If uranium uptake had occurred continuously after deposition, the U-series age should be younger than the EU-ESR age (*39, 42*). However, at Ngandong the U-series ages (Table 2) are all older than the EU-ESR age (Table 1). This pattern could be a result of leaching of uranium from the teeth late in their burial history, leaving the less soluble ^{230}Th behind, thus increasing the ^{230}Th/^{234}U and the U-series age. To test for this, we analyzed teeth from which we had removed outer layers of enamel of varying thickness. In all cases where outer (sediment-side) enamel layers were removed, the ages were less than or equal to the age of the whole enamel (Table 2). This result confirms that uranium has been leached from the outer part of the enamel late in its burial history, causing an increase in the ^{230}Th/^{234}U ratio (and thus the apparent U-series age) of the whole enamel. Removal of the outer layers of the tooth generally resulted in a slight decrease in the uranium concentration of the remaining material,

Table 1. ESR dates on fossil bovid teeth from Central Java. U-en, uranium concentration enamel; U-den, uranium concentration dentine. Uncertainty in uranium measurements are 1 ppm. EU and LU, uranium uptake modes; see text for full explanation. Neutron activation analysis yielded the following ranges of radioelements in the sediments from Ngandong: U − 1.13 to 1.56 (±0.1) ppm; Th − 4.41 to 6.27 (±0.17 to 0.36) ppm; and K − 0.52 to 0.73 (±0.3 to 0.4) % by weight.

Specimen number	Lab no.*	U-en (ppm)	U-den (ppm)	LU age (ka ± 1σ)	EU age (ka ± 1σ)
			Ngandong		
94NG-T1	95296A	6.2	186.4	48.1 ± 2.3	28.4 ± 1.3
	95296B	15.9	201.3	42.0 ± 2.5	24.1 ± 1.5
94NG-T2	95297A	11.9	192.2	48.6 ± 3.0	27.6 ± 1.7
	95297B	15.1	184.1	47.8 ± 3.1	27.0 ± 1.8
GRDC-1932	95393A	14.01	130.7	41.1 ± 4.8	23.7 ± 2.8
GDJM-1978	94762A	9.2	67.4	50.0 ± 5.8	30.4 ± 3.5
	Mean =			46.3 ± 3.7	26.9 ± 2.2
			Jigar		
	95301A	0.5	78.1	39.9 ± 3.0	27.2 ± 1.9
	95301B	0.6	87.7	39.7 ± 2.3	26.6 ± 1.4
	Mean =			39.8 ± 0.1	26.9 ± 0.4
			Sambungmacan		
(UGM-1973)	94761A	6.02	104.4	53.3 ± 4.0	32.4 ± 2.4

*A,B = samples prepared from different parts of the same tooth.

Table 2. U-Series dates on fossil bovid teeth from Ngandong, Central Java. All isotope ratios shown are activity ratios. Decay constant for ^{230}Th = 9.193 × 10^{-6} year^{-1}; ^{234}U = 2.833 × 10^{-6} year^{-1}. En, enamel; Den, dentine; ESD, micrometer's of enamel removed from outer (sediment) and inner (dentine) sides of tooth prior to dating. Uncertainties for uranium concentration, and ^{234}U/^{238}U, ^{230}Th/^{234}U, ^{230}Th/^{232}TH ratios are 2σ uncertainties in the last digits.

Material	ESD	U (ppm)	^{234}U/^{238}U	^{230}Th/^{234}U	^{230}Th/^{232}Th	Age ka ± 2σ
			94NG-T1 (95296)			
Den	n.a.	188(1)	1.042(6)	0.548(5)	9315(100)	85.8 ± 1.2
En1	0/0	11.92(5)	1.082(5)	0.350(2)	713(2)	46.6 ± 0.3
En2	51/54	11.16(3)	1.078(3)	0.316(5)	486(8)	41.1 ± 0.8
			94NG-T2 (95297)			
Den	n.a.	131(2)	1.07(13)	0.579(3)	3077(4)	92.8 ± 0.8
En1	0/0	17.12(7)	1.072(5)	0.30(1)	44(2)	37.6 ± 1.7*
En2	0/36	16.52(8)	1.084(5)	0.345(4)	111(1)	46.0 ± 0.7*
En5	69/0	17.56(8)	1.084(7)	0.317(8)	993(27)	41.3 ± 1.4
En4	29/0	15.78(8)	1.072(6)	0.271(5)	132(3)	33.8 ± 0.8*
			GRDC-1932 (95393)			
En1	0/0	15.62(9)	1.030(6)	0.298(3)	2689(25)	38.5 ± 0.4
En2	32/25	19.39(8)	1.042(4)	0.249(1)	3355(7)	31.0 ± 0.2
En3	73/65	8.34(3)	1.027(4)	0.26(1)	423(20)	32.0 ± 1.8*
En4	109/102	9.18(3)	1.034(4)	0.252(3)	1040(5)	31.5 ± 0.2

*Age corrected for detrital thorium.

even though we argue that the stripped (outer) portion had lost uranium. This effect is attributed to the original distribution of uranium in the teeth prior to uranium loss from the outer (surface) enamel. As observed by fission track mapping of uranium in teeth from other young sites, the concentration of uranium is typically highest near the enamel's outer surface and decreases inward (*38*).

The decrease in age after stripping of the outer surfaces of enamel agrees with U-series analyses of surface bone from Ngandong that indicate uranium loss (*26*). Stripping enamel from the inner (dentine) side of one sample (95297Den) yielded a higher age compared with the whole enamel age, possibly because of uptake from the uranium-rich dentine (Table 2). Analysis of the dentine from the Ngandong teeth gave apparent ages near 90 ka (Table 2). These old ages are similar to those obtained on bone (*26*), further confirming the greater tendency of dentine and bone to lose uranium compared to denser enamel.

Even though the U-series ages of the tooth enamel, after removal of the outermost enamel layer, approach the EU-ESR ages (*37*), this is not proof that the EU model correctly describes the uranium uptake history of the teeth. The stripping experiments show that there has been some increase in age as a result of uranium loss; however, we cannot be sure exactly how much increase has occurred. If the ages before uranium loss occurred were significantly lower than the EU-ESR age, then an LU model would be more appropriately applied to the ESR ages. A conservative conclusion from these experiments is that the true ages lie somewhere between the EU- and LU-ESR ages, but the complexities introduced by later uranium loss prevent a definitive assignment of an uranium uptake model. The EU and LU models give mean ESR ages of 27 ± 3 to 46 ± 4 ka for Ngandong, 27 ± 0.4 to 39.8 ± 0.1 ka for Jigar, and 27 ± 3 to 53 ± 4 ka for Sambungmacan (Table 1) (*37*), whereas our youngest U-series ages obtained from our Ngandong enamel stripping experiments was 31.0 ± 0.2 ka (Table 2).

The new dates from Ngandong and Sambungmacan are surprisingly young and, if proven correct, imply that *H. erectus* persisted much longer in Southeast Asia than elsewhere in the world. The youngest securely dated crania of African *H. erectus* come from Bed IV at Olduvai Gorge dated at older than 1 Ma (*43*), whereas the youngest mainland Asia *H. erectus* are older than 290 ka or 420 ka based on two U-series dating studies of the Layer 1-2 travertine at Zhoukoudian, China (*44–47*). Although the young ages for the Ngandong and Sambungmacan hominids might suggest that they should be grouped with early Australasian *H. sapiens* rather than with *H. erectus* (*1*), such an approach disregards morphological attributes unique to each of these groups of hominids. Although the Ngandong and Sambungmacan hominids possess a relatively large braincase for *H. erectus*, they retain Southeast Asian *H. erectus* autapomorphies, including cranial superstructures and vault shapes that distinguish them from the early Australasian *H. sapiens* (*3, 6, 48, 49*). On the other hand, the features shared by Ngandong *H. erectus* and the early Australasian *H. sapiens* are equally prevalent in fossil hominids from North Africa, suggesting that these features may be plesiomorphic (*49*).

If the Ngandong and Sambungmacan hominids represent a late-surviving sample of *H. erectus* (*50*), then the unilineal transformation in Southeast Asia from early and mid-Pleistocene *H. erectus* to the early Australasian *H. sapiens*—with Ngandong and Sambungmacan as intermediate steps, as proposed by the multiregional theory for the origin of *H. sapiens*—is no longer chronologically plausible. Rather, our ages for Ngandong and Sambungmacan indicate that *H. erectus* persisted in Southeast Asia into the latest Pleistocene overlapping in time with *H. sapiens* and raise the possibility that features shared by the two species are either homoplastic or the result of gene flow (*51*). In Africa and the Near East, *H. sapiens* first appear in the fossil record around 100 ka (*52*), and in mainland Asia perhaps by 67 ka (*45*). On Java, the oldest known *H. sapiens* date to less than 10 ka (*53*); however, evidence elsewhere in Southeast Asia indicates that *H. sapiens* arrived much earlier. Early *H. sapiens* date to about 30 ka in Australia (*54*) and possibly to 40 ka in Malaysia (*55*), whereas archaeological remains attributed to *H. sapiens* occur as early as 40 ka in New Guinea (*56*) and 50 ka (or greater) in Australia (*17, 57*). The temporal and spatial overlap between *H. erectus* and *H. sapiens* in Southeast Asia, as implied by our study, is reminiscent of the overlap of Neandertals (*H. neanderthalensis*) (*58*) and anatomically modern humans (*H. sapiens*) in Europe (*59*).

REFERENCES AND NOTES

1. M. H. Wolpoff, A. G. Thorne, J. Jelinek, Z. Yingun, *Cour. Forschungsinst. Senckenb.* **171**, 341 (1994).
2. A. G. Thorne and M. H. Wolpoff, *Am. J. Phys. Anthropol.* **55**, 337 (1981). Note, however, that Webb considers WLH-50 pathological [S. Webb, *Paleopathology of Aboriginal Australians: Health and Disease of a Hunter-Gatherer Continent* (Cambridge Univ. Press, Cambridge, 1995)].
3. G. P. Rightmire, *Cour. Forschungsinst. Senckenb.* **171**, 319 (1994).
4. C. B. Stringer and C. Gamble, *In Search of the Neanderthals* (Thames and Hudson, London, 1992); C. B. Stringer, in *Continuity or Replacement: Controversies in* Homo sapiens Evolution, G. Bräuer and F. H. Smith, Eds. (Balkema, Rotterdam, 1992), pp. 9–24.
5. G. Bräuer, in *Continuity or Replacement: Controversies in* Homo sapiens Evolution, G. Bräuer and F. H. Smith, Eds. (Balkema, Rotterdam, 1992), pp. 83–98.
6. A. P. Santa Luca, *Yale Univ. Publ. Anthropol. 78* (1980).
7. F. Weidenreich, *Anthropol. Pap. Am. Mus. Nat. Hist.* **43**, 205 (1951).
8. W. F. F. Oppenoorth, *Natur Mus.* **62**, 269 (1932); *Wet. Meded.* **20**, 49 (1932); *Kon. Ned. Aardr. Genootsch. Tijdschr.* **53**, 399 (1936); C. ter Haar, *Ing. Ned. Indië Mijning.* **4,** 51 (1934).
9. I. Moelyadi, *Proy. Penel. Paleoanthropol. Nas. Yogyak.*, (1982).
10. G.-J. Bartstra, S. Soegondho, A. van der Wijk, *J. Hum. Evol.* **17**, 325 (1988).
11. C. Swisher, personal field observation.
12. Personal observation of GRDC, and GMU museum collections by S. C. Antón and C. C. Swisher.
13. G. H. R. von Koenigswald, *Meeting Prehistoric Man* (Thames and Hudson, New York, 1956).
14. Unpublished notes, F. Weidenreich, in American Museum of Natural History, Department of Library Services.
15. F. Aziz, GRDC personal communication
16. G. H. R. von Koenigswald, *Ing. Ned. Indië Mijning.* **1,** 185 (1934).
17. R. Klein, *The Human Career* (Univ. of Chicago Press, Chicago, 1989).
18. Unpublished G. H. R. von Koenigswald photographs, Senckenberg Museum, Frankfurt Am Main, Germany.
19. A. Bartsiokas and M. H. Day, *Proc. R. Soc. London B* **252**, 115 (1993).
20. T. Jacob, in *Catalogue of Fossil Hominids, Part III: Americas, Asia, Australia*, K. P. Oakley, B. G. Campbell, T. I. Molleson, Eds. [British Museum (Natural History), London, 1975], pp. 103–115.
21. *F/P* = 0.06 for Ngandong calvaria V and *F/P* = 0.046 for nonhominid bone; *Catalogue of Fossil Hominids, Part III: Americas, Asia, Australia*, K. P. Oakley, B. G. Campbell, T. I. Molleson, Eds. [British Museum (Natural History), London, 1975].
22. M. Suzuki, Wikarno, Budisantoso, I. Saefundin, M. Itihara, in *Quaternary Geology of the Hominid Fossil Bearing Formations in Java*, N. Watanabe and D. Kadar, Eds. (Spec. Publ. 4, Geological Research and Development Centre, Bandung, Indonesia, 1985), pp. 309–358.
23. F. C. Howell, *L'Anthropologie* **90**, 447 (1986).
24. M. Itihara, T. Shibasaki, Sudijono, T. Hayashi, K. Furuyama, in (*22*), pp. 63–68.
25. G.-J. Bartstra, *Palaeohist. Gröningen* **29**, 1 (1987).
26. J. van der Plicht, A. van der Wijk, G. J. Bartstra, *Appl. Geochem.* **4**, 339 (1989).
27. A. Milard and R. Hedges, *Archaeol. Sci.* **22**, 200 (1995).
28. H. P. Schwarcz and B. Blackwell, in *Uranium Series Disequilibrium: Application to Environment Problems in Earth Science*, M. Ivanovich and R. S. Harmon, Eds. (Oxford Univ. Press, London, ed. 2, 1991), p. 513.
29. C.C. Swisher III, unpublished data.
30. R. Grün, H. P. Schwarcz, S. Zymela, *Can. J. Earth Sci.* **24**, 1022 (1987).
31. R. Grün and C. B. Stringer, *Archaeometry* **33**, 153 (1991).
32. The internal rates measured on the teeth are so high that the external dose as determined from the dosimeters will have no measurable affect on the calculated age.
33. G. Nitihaminoto and I. Moelyadi, *Pusat Penel. Purbak. Pening. Nas.*, 1–40 (1977).
34. T. Jacob, in *Homo erectus: Papers in Honor of Davidson Black*, B. A. Sigmon and J. S. Cybulski, Eds. (Toronto University Press, Toronto, 1981), pp. 87–104; S. Matsu‡ura, N. Watanabe, F. Aziz, T. Shibasaki, M. Kondo, *Bull. Nat. Sci. Mus. Tokyo Ser. D* (*Anthropol.*) **16**, 19 (1990).
35. G. P. Rightmire, *The Evolution of* Homo erectus (Cambridge Univ. Press, Cambridge, 1993).
36. W.-X. Li, J. Lundberg, A. P. Dickin, D. C. Ford, H. P. Schwarcz, *Nature* **339**, 534 (1989); W. J. Rink *et al.*,

J. Archaeol. Sci. **21**, 839 (1994).

37. Associated sediment collected less than 10 cm from the in situ teeth was collected for estimation of beta and gamma dose rates. We used the in-situ sediment collected near 95297 at Ngandong to estimate dose rates to museum teeth 94762 and 95393 from Ngandong, and 94761 from Sambungmacan. The internal dose rates for all teeth are high, and slight variations in the composition of enclosing sediment used for museum samples would have negligible effect on the calculated ages. The ESR ages (Table 1) were calculated using the standard program DATA of R. Grün. The ESR ages were also calculated using new ESR dating software called ROSY (B. J. Brennan, W. J. Rink, E. L. McGuirl, H. P. Schwarcz, W. V. Prestwich, *Radia. Meas.*, in press) using "One-Group" theory for beta dose attenuation in enamel. Using this method, both the EU- and LU-ESR ages are approximately 4000 years older than those using the DATA program. The mean EU age for Ngandong would be 31.4 ± 3.5 ka and agrees more closely with the U-series ages of 30 to 40 ka for the stripped enamels U-series ages.
38. C. R. McKinney, thesis, Southern Methodist University (1991).
39. R. Grün and F. McDermott, *Quat. Sci. Rev.* (*Quat. Geochronol.*) **13**, 121 (1994).
40. R. Grün and L. Taylor, *Ancient Thermolumia* **14**, 21 (1996).
41. R. Grün, H. P. Schwarcz, J. Chadam, *Nucl. Tracks* **14**, 237 (1988).
42. F. McDermott, R. Grün, C. B. Stringer, C. J. Hawkesworth, *Nature* **363**, 252 (1993).
43. E. Tamarat, N. Thouveny, M. Taieb, N. D. Opdyke, *Palaeogeogr. Palaeoclimatol. Palaeoecol.* **114**, 273 (1994).
44. C. Tiemei and Y. Sixun, *Archaeometry* **30**, 59 (1988).
45. Y. Sixun, C. Tiemei, G. Shijun, *Acta Anthropol. Sin.* **5**, 179 (1986); more recently, P. Brown [*Philos. Trans. R. Soc.* (1993)] has argued that there is no clear association of this date with the hominid skull at Liujiang.
46. Y. Sixun, C. Tiemei, G. Shijun, H. Yanqui, *Acta Anthropol. Sin.* **10**, 189 (1991).
47. S. Guanjun and J. Linhong, *ibid.*, p. 273; R. Ku, personal communication
48. S. C. Antón, in preparation; P. Brown, *Archaeol. Oceania* **16**, 156 (1981); *Terra Aust.* **13** (1989); N. W. G. Macintosh and S. L. Larnach, in *The Origin of the Australians*, R. L. Kirk and A. G. Thorne, Eds. (Humanities, Atlantic Highlands, NJ, 1976), p. 113; S. Webb, *Paleopathology of Aboriginal Australians: Health and Disease of a Hunter-Gatherer Continent* (Cambridge Univ. Press, Cambridge, 1995); N. W. G. Macintosh and S. L. Larnach, *Arch. Phys. Anthropal. Oceania* **7**, 1 (1972). and refs. 1 and 7 therein.
49. M. M. Lahr, *J. Hum. Evol.* **26**, 23 (1994).
50. F. C. Howell, in *Origins of Anatomically Modern Humans*, M. H. Nitecki and D. V. Nitecki, Eds. (Plenum, New York, 1994), p. 253.
51. J. H. Relethford and C. B. Stringer, in preparation.
52. H. P. Schwarcz and R. Grün, *Philos. Trans. R. Soc. London B* **337**, 145 (1992); H. Valladas *et al.*, *Nature* **331**, 614 (1988).
53. P. Storm, *Scri. Geol.* **110**, 1 (1996); R. Shutler, in *Felicitation for R. P. Soejdono*, in press.
54. J. M. Bowler, A. G. Thorne, H. A. Polach, *Nature* **240**, 48 (1972).
55. D. R. Brothweil, *J. Sarawak Mus.* **323**, 1 (1960). There appears to be some question as to whether the ^{14}C dates are physically related to the Niah Cave hominid remains.
56. L. Groube, J. Chappell, J. Muke, D. Price, *Nature* **324**, 453 (1986).
57. R. G. Roberts, R. Jones, M. A. Smith, *ibid.* **345**, 153 (1990); P. G. Bahn, *ibid.* **383**, 577 (1996); R. L. K. Fullager, D. M. Prince, L. M. Head, *Antiquity*, in press.
58. I. Tattersall and J. Schwartz, *Proc. Nat. Acad. Sci. U.S.A.*, in press.
59. Predecessors to Neandertals first appear by the Mid-Pleistocene in Western Europe [E. Carbonell *et al.*, *Science* **269**, 826 (1995); H. de Lumley and M.-A. de Lumley, *C. R. Acad. Sci. Paris* **272**, 1729 (1971)], whereas classical Neandertals persist until nearly 30 ka [J. K. Kozlowski, *Excavations in the Bacho Kiro Cave, Bulgaria* (*final report*) (Paristwowe Wydaruynictwo, Naukowe, Warsaw, 1982); J. L. Bischoff, N. Soler, J. Maroto, R. J. Julia, *J. Archaeol. Sci.* **16**, 553 (1989)], overlapping in time and space with anatomically modern humans that first appear in Europe and Western Asia around 40 to 50 ka [J. J. Hublin, C. Barroso Ruiz, P. Medina Lara, M. Fontugni, J.-L. Reyss, *C. R. Acad. Sci. Paris* **321**, 931 (1995); J. J. Hublin, F. Spoor, M. Braun, F. Zonneveld, S. Condemi, *Nature* **381**, 224 (1996); C. B. Stringer and R. Grün, *ibid.* **351**, 701 (1991); M. H. Wolpoff and D. Frayer, *ibid.* **356**, 200 (1992); D. Frayer, in *Continuity or Replacement: Controversies in* Homo sapiens Evolution, G. Bräuer and F. H. Smith, Eds. (Balkema, Rotterdam, 1992), pp. 179–188].

60. This project was supported by NSF (SBR-9405320) and L. S. B. Leakey Foundation grants to C.C.S. and G.H.C. Partial support for ESR and U-series dating was by NSF grant SBR-9410906 to H. Schwarcz; laboratory assistance was by K. Googer and J. Johnson. We would like to thank T. Jacob and F. Aziz for their help with field arrangements and museum specimens and C. B. Stringer, who provided valuable comments on an earlier draft of this manuscript.

26 June 1996; accepted 23 October 1996

Dynamical Signature of the Mott-Hubbard Transition in Ni(S,Se)$_2$

A. Husmann, D. S. Jin,* Y. V. Zastavker,† T. F. Rosenbaum,‡
X. Yao, J. M. Honig

The transition metal chalcogenide Ni(S,Se)$_2$ is one of the few highly correlated, Mott-Hubbard systems without a strong first-order structural distortion that normally cuts off the critical behavior at the metal-insulator transition. The zero-temperature (*T*) transition was tuned with pressure, and significant deviations were found near the quantum critical point from the usual $T^{1/2}$ behavior of the conductivity characteristic of electron-electron interactions in the presence of disorder. The transport data for pressure and temperature below 1 kelvin could be collapsed onto a universal scaling curve.

Disorder can turn a good metal into an insulator. Alternatively, strong interactions between electrons can split the half-filled band of a crystalline metal and open an insulating gap. In the first limit, a critical degree of disorder localizes the electrons through quantum interference and leads to the continuous Anderson transition at $T = 0$. In the correlation-driven scenario, a metal-insulator (MI) transition occurs when the ratio of the intrasite Coulomb repulsion to the bandwidth is of order unity. This Mott-Hubbard picture applies at nonzero temperature and is usually first order, often with coincident electronic, magnetic, and structural transitions.

This dichotomy between the Anderson and the Mott-Hubbard limits suffuses theoretical treatments of the MI transition (*1*). However, blending correlations and disorder can be more amenable to theoretical exposition, with the possibility of a well-defined order parameter (*2*). Experimental characterization of the critical behavior requires high-resolution measurements in the $T \rightarrow 0$ limit on materials that must satisfy a severe set of constraints: (i) true statistical disorder without the chemical segregation that gives rise to classical percolation effects; (ii) strong electron-electron interactions, but only a modest band gap to permit tuning; and (iii) strong electron-electron interactions, but no first-order structural instability at the MI transition.

It is this last constraint that may be the most restrictive in the highly correlated limit. For example, it is possible to deconvolute the effects of correlations and disorder at the $T = 0$ MI transition in the Mott-Hubbard system vanadium sesquioxide (*3*), but there are no actual divergences. The critical behavior at the transition is cut off by a sudden, symmetry-breaking, monoclinic distortion. In contrast, the transition-metal chalcogenide $NiS_{2-x}Se_x$ is one of the select few Mott-Hubbard materials (*4*) without a structural instability tied to the localization of charge (*5*). The $T = 0$ MI transition can be tuned with pressure, which offers an experimental approach to the mixture of statics and dynamics at a quantum critical point.

Nickel diselenide, $NiSe_2$, is a good metal while nickel disulfide, NiS_2, is a Mott insulator, whose half-filled narrow $3d$ e_g band is split by the Hubbard *U*, the intrasite Coulomb repulsion, with a band gap < 1 eV (*6*). Substitution of Se for S drives the system metallic, with a MI transition seen as a function of temperature for $NiS_{2-x}Se_x$ in the narrow range $0.47 < x <$

A. Husmann, D. S. Jin, Y. V. Zastavker, T. F. Rosenbaum, The James Franck Institute and Department of Physics, The University of Chicago, Chicago, IL 60637, USA.
X. Yao and J. M. Honig, Department of Chemistry, Purdue University, West Lafayette, IN 47907, USA.

*Present address: Joint Institute for Laboratory Astrophysics, University of Colorado, Boulder, CO 80309, USA.

†Present address: Department of Physics, Massachusetts Institute of Technology, Cambridge, MA 02139, USA.

‡To whom correspondence should be addressed.